

UC Davis

UC Davis Previously Published Works

Title

Loss of MXD3 induces apoptosis of Reh human precursor B acute lymphoblastic leukemia cells

Permalink

<https://escholarship.org/uc/item/1v82h9c4>

Journal

Blood Cells Molecules and Diseases, 54(4)

ISSN

1079-9796

Authors

Barisone, Gustavo A

Satake, Noriko

Lewis, Carly

et al.

Publication Date

2015-04-01

DOI

10.1016/j.bcnd.2014.12.002

Peer reviewed



Published in final edited form as:

Blood Cells Mol Dis. 2015 April ; 54(4): 329–335. doi:10.1016/j.bcmd.2014.12.002.

Loss of MXD3 Induces Apoptosis of Reh Human Precursor B Acute Lymphoblastic Leukemia Cells

Gustavo A. Barisone^{1,+}, Noriko Satake^{2,3,+}, Carly Lewis², Connie Duong², Cathy Chen², Kit S. Lam⁴, Jan Nolte³, and Elva Díaz^{1,*}

¹Department of Pharmacology, UC Davis School of Medicine, Davis and Sacramento, CA

²Department of Pediatrics, Hematology/Oncology section, UC Davis School of Medicine, Davis and Sacramento, CA

³Stem Cell Program and Institute of Regenerative Cures, UC Davis School of Medicine, Davis and Sacramento, CA

⁴Department of Biochemistry and Molecular Medicine, UC Davis School of Medicine, Davis and Sacramento, CA

Abstract

MXD3 is a transcription factor that plays an important role in proliferation of human DAOY medulloblastoma cells. Here, we demonstrate that MXD3 is highly enriched in human precursor B acute lymphoblastic leukemia (preB ALL) samples compared to mobilized peripheral blood mononuclear cells, bone marrow, or hematopoietic stem cells from healthy donors. MXD3 knock-down in the preB ALL cell line Reh resulted in decreased cell numbers with no change in G0/G1, S or G2/M populations but increased apoptosis compared to control cells. Our results suggest that MXD3 is important for survival of Reh preB ALL cells, possibly as an anti-apoptotic factor.

Keywords

precursor B acute lymphoblastic leukemia; proliferation; MXD3; apoptosis

INTRODUCTION

Leukemia is the most common cancer in children. Precursor B acute lymphoblastic leukemia (preB ALL) is the most prevalent phenotype [1]. Recent therapeutic advances have made ALL highly curable (89% survival rate). However, a subset of childhood ALL cases

© 2014 Elsevier Inc. All rights reserved.

*Correspondence to: E. Diaz, Department of Pharmacology, 451 Health Sciences Drive, 3503 Genome & Biomedical Sciences Facility, UC Davis School of Medicine, Davis, CA 95616; ediaz@ucdavis.edu; Phone: (530) 754-6080; Fax: (530) 754-7393.

⁺Equal contribution

CONFLICT OF INTEREST STATEMENT

The authors have declared that no competing interests exist.

Publisher's Disclaimer: This is a PDF file of an unedited manuscript that has been accepted for publication. As a service to our customers we are providing this early version of the manuscript. The manuscript will undergo copyediting, typesetting, and review of the resulting proof before it is published in its final citable form. Please note that during the production process errors may be discovered which could affect the content, and all legal disclaimers that apply to the journal pertain.

continues to have poor prognosis, with survival rates as low as 30% [2]. Furthermore, current standard treatment consists of combination chemotherapy that is highly toxic to growing children, both in short and long terms [3, 4]. Unlike childhood cases, the survival rate for adult ALL remains low, although recent advances in therapy are promising [5]. To improve survival rates in groups with poor prognosis and to avoid serious side effects, new approaches are needed that specifically target leukemia cells.

MXD3 is a member of the MXD family of basic-helix-loop-helix transcription factors [6] that form heterodimers with the cofactor MAX [7, 8], and were originally proposed as functional antagonists of MYC proteins in the MYC/MAX/MAD transcriptional network [6, 9–12]. While some MXD proteins are MYC antagonists by acting as transcriptional repressors to promote cell differentiation [7, 9, 11, 13], MXD3 is an atypical member that plays a role in proliferation rather than differentiation [6, 14–18]. MXD3 promotes granule neuron precursor (GNP) proliferation through a Sonic Hedgehog-mediated pathway [17], it is expressed in a mouse model of medulloblastoma [17], and its knock-down (KD) reduced proliferation of the human medulloblastoma cell line DAOY [18]. Since MXD3 appears to be associated with a variety of human cancers [15] and pathways related to B cell malignancies [19, 20], we investigated the role of MXD3 in preB ALL. Here we report the high expression of MXD3 in primary human preB ALL samples and cell lines and demonstrate that MXD3 is important for leukemia cell survival in preB ALL, possibly as an anti-apoptotic factor.

MATERIALS AND METHODS

Primary cells and cell lines

Primary patient samples or human samples harvested from mice were used in this study. All of the leukemia samples except two samples were obtained from pediatric patients at diagnosis, with informed written consent using the UC Davis Institutional Review Board (IRB) approved protocol # 230971-2. Written informed consent was obtained from patients or their caretakers (if they were minors). The samples were de-identified upon collection per protocol. Two samples were obtained as anonymized discarded samples under IRB guidelines. Leukemia mouse xenograft models were established (Satake, manuscript in preparation) using the procedure “serial transplantation of leukemia cells” approved under IACUC protocol # 17722 (PI: Kit Lam). Human peripheral blood mononuclear cells (PBMC) and bone marrow (BM) cells were obtained from the UC Davis Stem Cell Transplant Program as anonymized discarded samples with a formal waiver from the IRB allowing us to use the de-identified discarded samples without the original patients’ consent. The UC Davis IRB approved this study. Cells were isolated by centrifugation through a Ficoll gradient and frozen with 10% DMSO in liquid nitrogen until use. Cell lines were obtained from ATCC (Reh and JM1) and the Lam lab (Jurkat), and cultured in RPMI 1640 medium (Invitrogen) supplemented with 10% fetal bovine serum (Gibco), 140 mM glucose, 1 mM sodium pyruvate, 1mM Hepes, 100 U/mL penicillin and 100 µg/mL streptomycin in a humidified incubator at 37°C and 5% CO₂. Cells were split 1:10 before cultures reached a density of 2×10⁶ cells/ml. All procedures involving human or animal samples were performed under approved protocol following federal, state and institutional guidelines.

Quantitative PCR

Cells were collected by centrifugation (200 \times g, 7 minutes, room temperature) and resuspended (without washing) in lysis buffer. RNA was isolated using the RNeasy mini kit (Qiagen). Following purification, up to 7 μ g total RNA were digested with DNase using Turbo DNA-free (Ambion) according to the manufacturer's instructions to remove traces of genomic DNA. Up to 1 μ g of DNase-treated RNA was reverse-transcribed into cDNA using the High Capacity RNA to cDNA kit (Applied Biosystems). Quantitative PCR (qPCR) was performed in a 7900HT system using a validated MXD3 Taqman assay (Hs01557564_m1, Applied Biosystems) and TaqMan master mix. Triplicate 12 μ l reactions were performed with 50 ng cDNA template per reaction in 384-well plates. Negative controls included no-reverse transcriptase reactions and water-only reactions. Relative expression levels were calculated by the comparative C_T method, using 18S RNA as an endogenous control, also run in triplicate with the appropriate negative controls. Data were analyzed using SDS and DataAssist software. All qPCR reagents, instrument and software were from Applied Biosystems.

Immunoblotting and Immunocytochemistry

Total protein extracts in RIPA buffer (150 mM NaCl, 1% Na deoxycholate, 0.1% SDS, 1% Triton X-100, 50 mM Tris, pH 7.2) were subject to 12% denaturing SDS-PAGE and transferred to nitrocellulose. Blots were blocked in 5% non-fat dry milk (NFDM) in PBS for at least 1 hour at room temperature, incubated with primary antibodies in 5% NFDM in PBS with 0.01% Tween-20 (PBST) overnight at 4°C, washed 3 times, 10 minutes each with PBST, incubated with secondary antibodies for 45 minutes at room temperature and washed again as above. Blots were imaged using an infrared scanner (Li-Cor Biosciences). Primary antibodies were as follows: mouse anti-MXD3 (NeuroMab clone N129/15) 1:1,000; mouse anti-histone3 (Millipore) 1:10,000. Secondary antibody was goat anti-mouse IRDye 800CW (Li-Cor) 1:10,000.

For immunocytochemistry, cells were collected and fixed with 10% buffered formalin for 10 min before washing in PBS, then smeared and air-dried on slides for immunofluorescence. For antigen retrieval, slides were incubated in a citrate buffer (10 mM sodium citrate, 0.05% Tween, pH 6) for 10 min at 95°C. Slides were then blocked at room temperature with 0.2% Triton-X100, 10% FBS in PBS for 15 min, followed by 10% FBS in PBS for another 15 min. Slides were incubated with anti-MXD3 antibodies diluted in 1%FBS/PBS at a final concentration of 2 μ g/mL overnight at 4 °C. After washing 3 times in PBS at room temperature, a secondary goat anti-mouse antibody conjugated to AlexaFluor 488 (Invitrogen) was added at a concentration of 4 μ g/mL for 3 hrs at room temperature) and washed as above. DAPI was used for nuclei staining.

Viral constructs and transduction

Lentiviral shuttle vectors for MXD3 knock-down (shMXD3) or negative control (shCTRL) were generated by annealing and ligating oligonucleotides in HpaI/XhoI in the pLB backbone. Oligonucleotides were annealed by heating a 50 μ M (each) solution to 95°C and then left to cool to room temperature in a beaker containing 300 ml of water previously heated to 85°C. Annealed oligonucleotides were phosphorylated with T4 polynucleotide

kinase for 30 minutes at 37°C and then ligated into pLB previously digested with HpaI/XhoI and dephosphorylated. Oligonucleotides were designed so that an XhoI overhang was left at the 3' end after annealing. Oligonucleotides used were: shMXD3, 5'-TGA CTG TGC CCG GTA CAC CAT TCA AGA GAT GGT GTA CCG GGC ACA GTC TTT TTT C-3' and 5'-TCG AGA AAA AAG ACT GTG CCC GGT ACA CCA TCT CTT GAA TGG TGT ACC GGG CAC AGT CA-3'; shCTRL, 5'-TTG TGT GCA CAC ACG CGC ACT TCA AGA GAG TGC GCG TGT GTG CAC ACA TTT TTT C-3' and 5'-TCG AGA AAA AAT GTG TGC ACA CAC GCG CAC TCT CTT GAA GTG CGC GTG TGT GCA CAC AA-3'. To generate a rescue construct, HA-tagged MXD3 cDNA was mutagenized using the QuikChange II XL (Agilent Technologies) to introduce silent mutations within the siRNA target sequence (5'-GAC TGT GCC CGG TAC ACC A-3' to 5' GATGcGCaCGc At ACg A-3'), thereby resulting in a message that was insensitive to shRNA-mediated KD while still coding for the wild-type protein. An internal ribosome entry site (IRES) sequence was cloned immediately upstream of mutagenized MXD3. The fusion IRES-MXD3 was cloned immediately downstream of the EGFP coding sequence in pLB-shMXD3 using EcoRI sites. Hence, this rescue construct was expected to KD endogenous MXD3 and express the vector-coded, wild-type (HA-tagged) protein and free GFP. Mutagenic primers, designed with Agilent's QuikChange Primer Design Application, were 5'-TGC CCC TGG GGG CCG ATT GCG CAC GCT ATA CGA CGC TGA GCC TG-3' and 5'-CAG GCT CAG CGT CGT ATA GCG TGC GCA ATC GGC CCC CAG GGG CA-3'.

Recombinant lentiviruses were produced by transfecting 2.4×10^7 HEK293T cells in a T225 flask (Corning) with 25 µg of the shuttle vector, 25 µg of the packaging plasmid (8.2) and 5 µg of the pseudotyping vector (pVSVG) with 130 µl of TransIT-293 transfection reagent (Mirus Bio) according to the manufacturer's instructions, in a final culture volume of 29 ml. After overnight incubation, the transfection medium was discarded and replaced with 35 ml of Ultraculture medium (Lonza) without any additives. Culture supernatants were collected 48 hours later, filtered through a 0.45 µm PVDF vacuum-drive device (Millipore) and concentrated with a Centricon Plus-70 filter unit (Millipore) as per the manufacturer's instructions. Concentrated lentiviruses were aliquoted and stored at -80°C. To determine viral titers, 5×10^5 COS cells/well in 6-well plates were infected (in duplicate) with serial dilutions of the lentivirus stock for 3 hours at 37°C. Virus titers were estimated 72 hours after infection by flow cytometry, using the GFP reporter coded in the shuttle vector. Typical titers were 1.5×10^8 TU/ml.

Lentiviral particles were added to 0.5×10^6 Reh cells in 2.5 ml medium at multiplicity of infection (MOI) = 10, with 2 µg/ml polybrene and incubated overnight. Efficiency of transduction was measured by flow cytometry for GFP expression (coding sequence present in all constructs) 3 days after transduction.

Cell proliferation, apoptosis and cell cycle

Aliquots were taken at specified times and viable cells counted in a hemacytometer using Trypan Blue stain. Three independent experiments were performed, each in triplicate. Statistical analysis was performed using Prism 5 software (Graphpad Prism, Inc).

For apoptosis analysis, cells were collected by centrifugation and washed with Hanks Buffered Salt Solution (HBSS, Gibco) before staining with the Vybrant DyeCycle/Sytox AADvance kit (Invitrogen) according to the manufacturer's instructions. Flow cytometry was performed in a Becton-Dickinson LSRII instrument. Data (50,000 events/sample) were analyzed with Cyflogic (CyFlo Ltd., Finland).

For cell cycle analysis, cells were washed and resuspended in PBS and fixed with 70% ethanol at -20°C overnight. Cell pellets were washed with PBS, resuspended in 20 $\mu\text{g}/\text{mL}$ propidium iodide, 0.1% Triton X-100, 200 $\mu\text{g}/\text{mL}$ RNase A in PBS and incubated for 30 minutes at room temperature. Data were acquired with a Becton-Dickinson FacScan instrument and fitted with ModFit.

Statistical analysis

Results were analyzed by ANOVA with Bonferroni post tests for statistical comparison. Results were considered to be significantly different when $p < 0.05$. All statistical analysis was performed using Graphpad Prism software.

RESULTS

MXD3 is highly expressed in preB ALL cells

Our cohort included a total of 11 human leukemia samples: 6 patient samples were frozen immediately after collection (ALL-1 to 6), and 5 patient samples were propagated as mouse xenograft (ALL-xeno-7 to 11). In all samples, *MXD3* was significantly elevated, with levels 15–30-fold higher than normal peripheral blood mononuclear cells (PBMCs) or bone marrow (BM) by quantitative real-time PCR (qPCR). We also observed high levels of *MXD3* in the preB ALL cell lines Reh and JM1, but not in the T-cell ALL cell line Jurkat (Fig. 1A, C). *MXD3* was low in PBMCs and BM samples (Fig. 1A) and isolated CD34(+) hematopoietic stem cells (not shown) from healthy donors. Immunoblot and immunocytochemistry analysis confirmed *MXD3* protein expression in a subset of leukemia samples tested but not in normal samples (Fig. 1B–C), validating the qPCR results. *MXD3* is expressed in normal B cells; however, its expression level was less than half of those in preB ALL cells (Satake et al., *in press*).

MXD3 KD reduces Reh cell number

To investigate a role for *MXD3* in leukemia proliferation we utilized Reh cells, which had levels of *MXD3* comparable to primary samples (Fig. 1). ALL cells are notoriously difficult to transfect (chemical transfection, lipofection and electroporation resulted in near 0% transfection efficiency, data not shown). Therefore, we used lentiviral-mediated transduction; as shown in Figure 2A, transduction was highly efficient with 84–91% of cells transduced with all constructs used in subsequent experiments. As shown in Table 1, the high efficiency of lentiviral transduction was consistent in five independent experiments. To confirm KD, transduced cells were analyzed by immunoblot. As shown in Figure 2B, transduction with *MXD3* shRNA (sh*MXD3*) resulted in markedly decreased *MXD3* levels compared with control shRNA (shCTRL) that does not target any human sequence. A rescue

construct expressed HA-tagged MXD3 (HA-MXD3) that was insensitive to shMXD3 at levels similar to the endogenous protein (Fig. 2B).

MXD3 KD led to a significant reduction in cell numbers when compared to shCTRL or non-transduced (NT) cells with statistically significant differences observed 4 days after transduction (Fig. 3). Transduction with the rescue construct (KD of the endogenous protein and expression of HA-MXD3) resulted in cell numbers restored to control levels (Fig. 3), indicating that the phenotype observed was due to MXD3 KD.

Effect of MXD3 KD on cell cycle and apoptosis in Reh cells

To investigate the MXD3 KD phenotype, we evaluated cell cycle progression by flow cytometry of propidium-iodide stained cells 5 days after KD, when cell numbers were already significantly lower than controls (Fig. 3). Under these conditions, we observed no differences in the percentage of cells in G0/G1, S or G2/M between KD and control samples (Fig. 4). However, MXD3 KD resulted in a significant increase in the apoptotic population and a decrease in the viable population as measured by flow cytometry with Vybrant DyeCycle/Sytox-stained samples (Fig. 5). Therefore, our results suggest that the reduced cell numbers observed are not due to cell cycle blockade but rather to increased cell death.

In previous work, we showed that MXD3 regulates MYC expression to promote cerebellar GNP proliferation [17]. However, MXD3 KD in Reh cells did not affect MYC levels (Relative MYC mRNA level compared to NT cells: shMXD3: 1.54 ± 0.2 ; shCTRL: 1.36 ± 0.12 ; shMXD3+Rescue: 0.91 ± 0.07).

DISCUSSION

The results presented here suggest that MXD3 may be involved in leukemia biogenesis and/or maintenance, consistent with our reported proliferative role for MXD3 in cerebellum [17] and its overexpression in cerebellar tumors [18]. MXD3 is expressed in transitional IgD⁻ B cells in the spleen, and its expression is reduced during maturation in mice [20]. It is possible then that the high MXD3 levels in preB ALL samples reflect the immature nature of leukemia cells. However, the observation of a reduced cell number phenotype upon KD suggests that MXD3 is actively involved in proliferation. MXD3 KD resulted in 50% reduction in cell numbers when compared to controls. However, it should be noted that ~10% of the cells were not transduced. Therefore, it is possible that the cells that continue to proliferate are those in which MXD3 has not been knocked down at all or incompletely knocked down. Intriguingly, MXD3 might act as an anti-apoptotic factor in leukemia cells, since an increase in the apoptotic population without a change in cell cycle progression was observed with MXD3 KD.

Previously, we demonstrated that MXD3 regulates MYC expression during Sonic Hedgehog-dependent cerebellar GNP proliferation [17]; however, we did not find any change in MYC level upon MXD3 KD in Reh cells. One possibility is that MXD3 is downstream of MYC in Reh cells; therefore, altering MXD3 levels would not be expected to impact MYC. Alternatively, MXD3 and MYC might be in separate pathways.

In summary, we showed that MXD3 is highly expressed in preB ALL cells when compared to normal hematopoietic cells, and that its KD in Reh cells results in decreased cell counts presumably due to apoptosis. While more experiments are needed to understand the mechanism of MXD3 function in leukemia, we propose that MXD3 KD may constitute an alternative or addition to conventional ALL therapy.

Acknowledgments

The authors wish to thank Drs. Qizhi Gong and Huaiyang Chen for their help with lentivirus production, Drs. Janet Yoon, Jong Chung, Jay Balagtas, and Anjali Pawar for assisting with primary sample collections, and Tin Ngo for assisting with proliferation assays. This work was supported by grants to N.S. from the Hartwell Foundation and the National Center for Advancing Translational Sciences, National Institutes of Health (NIH; UL1 TR000002), and to E.D. from the NIH Director's New Innovator Program (DP2 OD006479-01).

References

1. Pui CH, et al. Pediatric acute lymphoblastic leukemia: where are we going and how do we get there? *Blood*. 2012; 120(6):1165–74. [PubMed: 22730540]
2. Pui CH, Robison LL, Look AT. Acute lymphoblastic leukaemia. *Lancet*. 2008; 371(9617):1030–43. [PubMed: 18358930]
3. Bhatia S. Late effects among survivors of leukemia during childhood and adolescence. *Blood Cells Mol Dis*. 2003; 31(1):84–92. [PubMed: 12850490]
4. Robison LL. Late effects of acute lymphoblastic leukemia therapy in patients diagnosed at 0–20 years of age. *Hematology Am Soc Hematol Educ Program*. 2011; 2011:238–42. [PubMed: 22160040]
5. Ribera JM. Advances in acute lymphoblastic leukemia in adults. *Curr Opin Oncol*. 2011; 23(6):692–9. [PubMed: 21892082]
6. Hurlin PJ, et al. Mad3 and Mad4: novel Max-interacting transcriptional repressors that suppress c-myc dependent transformation and are expressed during neural and epidermal differentiation. *Embo J*. 1995; 14(22):5646–59. [PubMed: 8521822]
7. Ayer DE, Kretzner L, Eisenman RN. Mad: a heterodimeric partner for Max that antagonizes Myc transcriptional activity. *Cell*. 1993; 72(2):211–22. [PubMed: 8425218]
8. Ayer DE, Lawrence QA, Eisenman RN. Mad-Max transcriptional repression is mediated by ternary complex formation with mammalian homologs of yeast repressor Sin3. *Cell*. 1995; 80(5):767–76. [PubMed: 7889570]
9. Ayer DE, Eisenman RN. A switch from Myc:Max to Mad:Max heterocomplexes accompanies monocyte/macrophage differentiation. *Genes Dev*. 1993; 7(11):2110–9. [PubMed: 8224841]
10. Eisenman, RNE. *Current Topics in Microbiology and Immunology*. Vol. 302. Berlin: Springer; 2006. *The Myc/Max/Mad Transcription Factor Network*.
11. Foley KP, et al. Targeted disruption of the MYC antagonist MAD1 inhibits cell cycle exit during granulocyte differentiation. *Embo J*. 1998; 17(3):774–85. [PubMed: 9451002]
12. Grandori C, et al. The Myc/Max/Mad network and the transcriptional control of cell behavior. *Annu Rev Cell Dev Biol*. 2000; 16:653–99. [PubMed: 11031250]
13. Queva C, et al. Sequential expression of the MAD family of transcriptional repressors during differentiation and development. *Oncogene*. 1998; 16(8):967–77. [PubMed: 9519870]
14. Fox EJ, Wright SC. S-phase-specific expression of the Mad3 gene in proliferating and differentiating cells. *Biochem J*. 2001; 359(Pt 2):361–7. [PubMed: 11583582]
15. Barisone GA, Yun JS, Diaz E. From cerebellar proliferation to tumorigenesis: new insights into the role of Mad3. *Cell Cycle*. 2008; 7(4):423–7. [PubMed: 18235219]
16. Diaz E, et al. Molecular analysis of gene expression in the developing pontocerebellar projection system. *Neuron*. 2002; 36(3):417–34. [PubMed: 12408845]
17. Yun JS, et al. A novel role of the Mad family member Mad3 in cerebellar granule neuron precursor proliferation. *Mol Cell Biol*. 2007; 27(23):8178–89. [PubMed: 17893326]

18. Barisone GA, et al. Role of MXD3 in proliferation of DAOY human medulloblastoma cells. *PLoS One*. 2012; 7(7):e38508. [PubMed: 22808009]
19. Queva C, et al. Targeted deletion of the S-phase-specific Myc antagonist Mad3 sensitizes neuronal and lymphoid cells to radiation-induced apoptosis. *Mol Cell Biol*. 2001; 21(3):703–12. [PubMed: 11154258]
20. Gore Y, et al. Mad3 negatively regulates B cell differentiation in the spleen by inducing Id2 expression. *Mol Biol Cell*. 2010; 21(11):1864–71. [PubMed: 20375148]

Author Manuscript

Author Manuscript

Author Manuscript

Author Manuscript

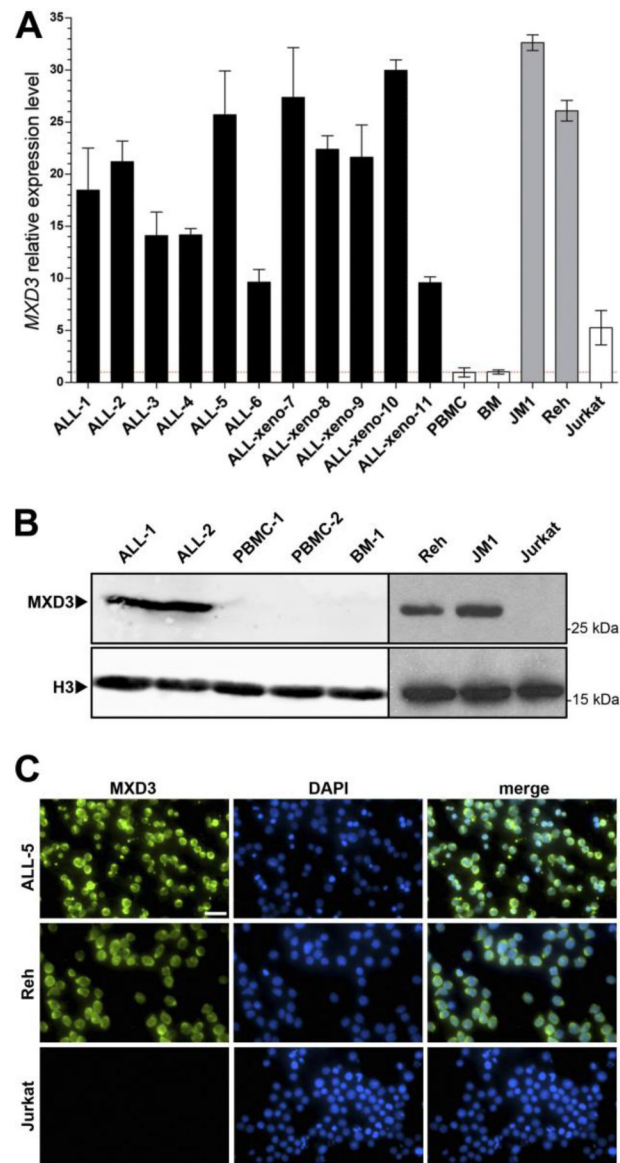


Figure 1. MXD3 is expressed in preB ALL but not in normal hematopoietic cells qPCR (A), immunoblot (B) and immunocytochemistry (C) showing high levels of MXD3 in preB ALL samples but not in normal cells. MXD3 message and protein were also high in the preB ALL cell line Reh, but not in the T-cell ALL line Jurkat. Bars represent the average \pm SD; all leukemia samples were significantly higher than normal controls ($p < 0.01$, ANOVA). Histone H3 was used as a load control, DAPI was used for nuclear stain.

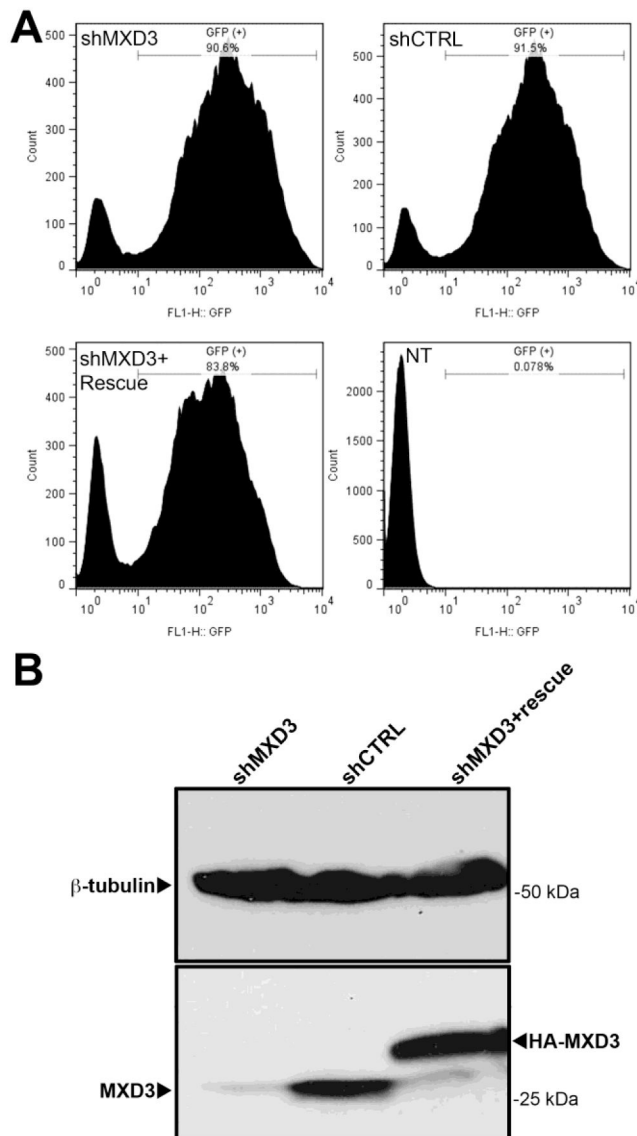


Figure 2. MXD3 is knocked-down efficiently by lentiviral transduction
(A) 84–91% efficiency was observed for lentiviral transduction of Reh cells. Data are representative of at least 5 experiments. **(B)** Reduced protein levels and rescue construct expression was confirmed by immunoblot.

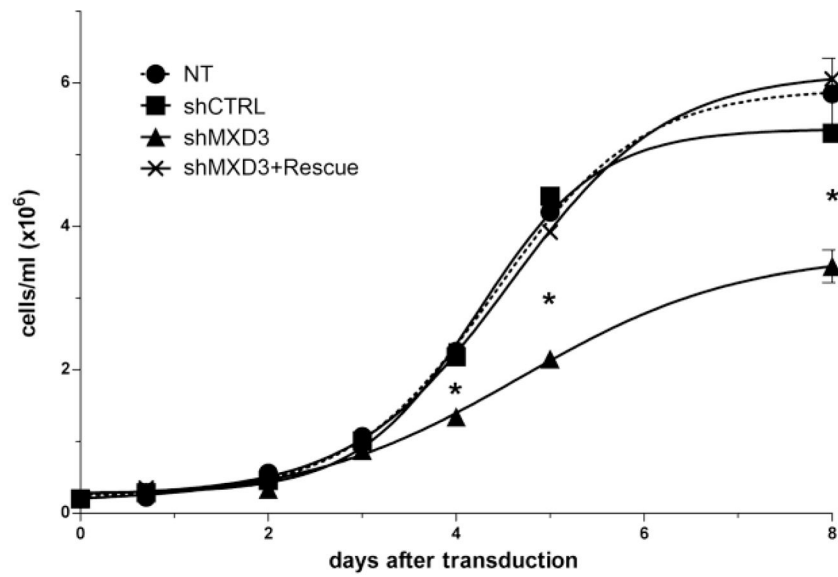


Figure 3. MXD3 knock-down reduces preB ALL cell proliferation

MXD3 knock-down in Reh (▲, shMXD3) resulted in decreased cell numbers when compared to a negative control shRNA (■, shCTRL) or non-transduced cells (●, NT). Simultaneous knock-down and expression of MXD3 restored cell numbers to basal levels (×, shMXD3+rescue). Experiments were performed in triplicate; error bars represent standard deviation (* $p < 0.001$, 2-way ANOVA with Bonferroni post-test).

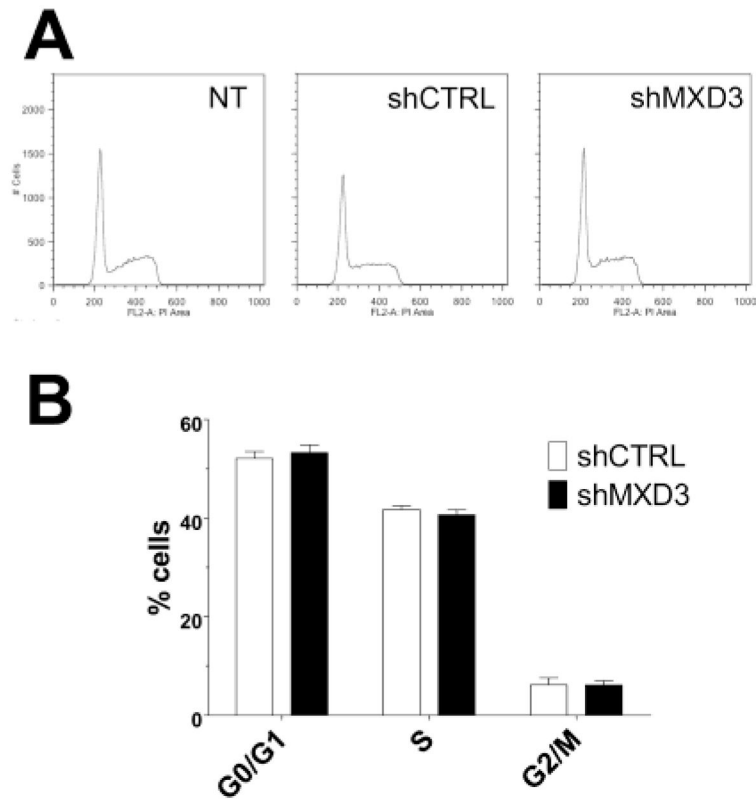


Figure 4. MXD3 knock-down does not induce cell cycle arrest

(A) Cell cycle analysis by flow cytometry of propidium iodide stained cells; 30,000 event were acquired. Histograms are representative of 3 independent experiments. (B) Percentage population of cells in the different stages of the cell cycle as assessed by propidium iodide staining. No statistically significant differences were observed between MXD3 knock-down (shMXD3, black bars) and control shRNA (shCTRL, white bars)-transduced Reh cells.

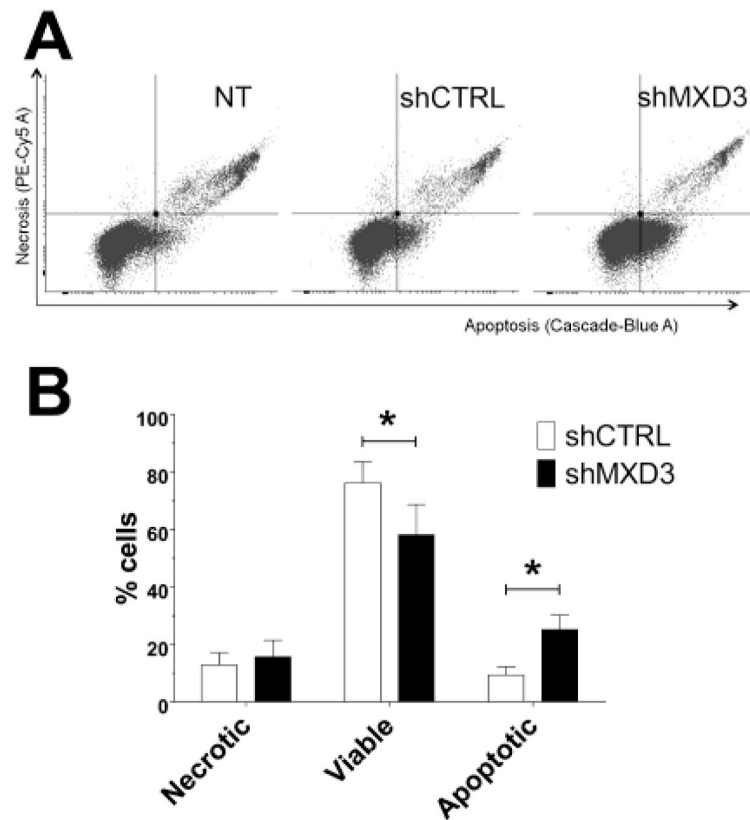


Figure 5. MXD3 knock-down increases apoptosis

(A) Transduced Reh cells stained for apoptosis with Vybrant® DyeCycle™ Violet stain (x axis, Cascade Blue channel) and SYTOXR AADvanced™ (y axis, PE-Cy5 channels). Flow cytometry scatter plots are representative of 3 independent experiments; 50,000 events were acquired in each experiment. (B) MXD3 knock-down resulted in a significant increase of apoptotic cells (lower right quadrant in A) and decrease in viable (lower left quadrant in A) cells in the population (n = 3, p < 0.05, 2-way ANOVA with Bonferroni post-test).

TABLE 1Transduction efficiency in Reh cells (%)^{*}

	shMXD3	shCTRL	shMXD3+rescue	NT
Experiment 1	85.8	88.1	80.3	0.07
Experiment 2	90.6	91.5	83.8	0.08
Experiment 3	89.3	88.5	79.2	0.13
Experiment 4	90.0	91.5	82.2	0.07
Experiment 5	84.7	89.6	78.8	0.07
Average ± SD	88.08 ± 2.65	89.84 ± 1.61	80.86 ± 2.11	0.08 ± 0.03

^{*}Data are reported as percentage of GFP(+) cells 72 hours after transduction as determined by flow cytometry.

Abbreviations: NT, not transduced; SD, standard deviation.

Author Manuscript

Author Manuscript

Author Manuscript

Author Manuscript